RhoG Promotes Neural Progenitor Cell Proliferation in Mouse Cerebral Cortex

Satoshi Fujimoto, Manabu Negishi, and Hironori Katoh

Laboratory of Molecular Neurobiology, Graduate School of Biostudies, Kyoto University, Sakyo-ku, Kyoto 606-8501, Japan

In early cortical development, neural progenitor cells (NPCs) expand their population in the ventricular zone (VZ), and produce neurons. Although a series of studies have revealed the process of neurogenesis, the molecular mechanisms regulating NPC proliferation are still largely unknown. Here we found that RhoG, a member of Rho family GTPases, was expressed in the VZ at early stages of cortical development. Expression of constitutively active RhoG promoted NPC proliferation and incorporation of bromodeoxyuridine (BrdU) in vitro, and the proportion of Ki67-positive cells in vivo. In contrast, knockdown of RhoG by RNA interference suppressed the proliferation, BrdU incorporation, and the proportion of Ki67-positive cells in NPCs. However, knockdown of RhoG did not affect differentiation and survival of NPC. The RhoG-induced promotion of BrdU incorporation required phosphatidylinositol 3-kinase (PI3K) activity but not the interaction with ELMO. Taken together, these results indicate that RhoG promotes NPC proliferation through PI3K in cortical development.

INTRODUCTION

In mammalian brain, cerebral cortex is highly organized, and its proper development is necessary for higher brain functions. Cortical neurons are generated in the ventricular zone (VZ) and sequentially migrate toward the pial side of cortex from the VZ to the cortical plate (CP) through the intermediate zone (IZ) to form six cell layers (Gupta *et al.,* 2002). In early stages of cortical development, the VZ is abundant in neural progenitor cells (NPCs), whose proliferative activity is spatially and temporally controlled by various molecules including cell cycle regulators, transcription factors, and extracellular factors (Götz and Huttner, 2005; Dehay and Kennedy, 2007). To date, a large number of studies have shown the process of neurogenesis and the molecular involvement in it, but intracellular signal transduction pathways regulating NPC proliferation remain largely unknown.

The Rho family small GTPases have been already known to be involved in various cellular functions such as cell migration, neurite extension, cell cycle progression, and cell division (Etienne-Manneville and Hall, 2002; Jaffe and Hall, 2005). Like other small GTPases, Rho family GTPases act as molecular switches by cycling between an inactive GDP-bound state and an active GTP-bound state, and activated GTPases can interact with their specific effectors. Rho family GTPases have been also suggested to be involved in various

stages of nervous system development including neuronal migration, neurite outgrowth, axon guidance, and synaptogenesis (Luo, 2000; Negishi and Katoh, 2002; Govek *et al.,* 2005). In the past few years, several lines of in vivo analyses have revealed the involvement of Rho family GTPases in early cortical development. For example, experiments using in vivo electroporation with constitutively active or dominant negative mutants show that Rac1 and Cdc42 are involved in radial migration of cortical neurons (Kawauchi *et al.,* 2003; Konno *et al.,* 2005). An analysis of Rac1 conditional knockout mice shows that Rac1 controls the formation of midline commissures and the competency of tangential migration in ventral telencephalic neurons, and the mice also show the neural progenitor reduction and microcephaly (Chen *et al.,* 2007, 2009). On the other hand, two distinct analyses of Cdc42 conditional knockout mice show that Cdc42 regulates NPC fate at the apical surface (Cappello *et al.,* 2006) and Cdc42 deficiency causes holoprosencephaly (Chen *et al.,* 2006). In addition, Rnd2, a member of Rho family GTPases that is predominantly expressed in brain, regulates the migration and morphological changes of cortical pyramidal neurons (Nakamura *et al.,* 2006; Heng *et al.,* 2008).

RhoG, a member of Rho family GTPases, was originally identified as a product of growth-stimulated genes in fibroblast (Vincent *et al.,* 1992). Previous studies have shown that RhoG is involved in diverse cellular functions by regulating cytoskeletal reorganization in various types of cells, including the regulation of neurite outgrowth in neuronal cells (Katoh *et al.,* 2000, Katoh and Negishi, 2003), cell migration (Hiramoto *et al.,* 2006; Katoh *et al.,* 2006a, Meller *et al.,* 2008), macropinocytosis in fibroblasts (Ellerbroek *et al.,* 2004), and phagocytosis of apoptotic cells (deBakker *et al.,* 2004; Nakaya *et al.,* 2006). In addition, RhoG is also involved in Ras-induced focus formation (Roux *et al.,* 1997), gene expression (Vigorito *et al.,* 2003), and cell survival (Murga *et al.,* 2002; Yamaki *et al.,* 2007). Northern blot analyses have shown that RhoG is expressed in the various tissues (Vincent *et al.,* 1992) includ-

Abbreviations used: BrdU, bromodeoxyuridine; CP, cortical plate; IZ, intermediate zone; NPC, neural progenitor cell; PI3K, phosphatidylinositol 3-kinase; shRNA, short hairpin RNA; SVZ, subventricular zone; VZ, ventricular zone.

ing the brain during development (Ishikawa *et al.*, 2002). However, little has known about the physiological functions of RhoG.

In this study, we attempted to reveal the role of RhoG in brain development, particularly focusing on the cerebral cortex. Because RhoG was expressed in the developing VZ, which is abundant in NPCs, we utilized in vivo electroporation to examine the NPC-specific functions of RhoG and showed a novel function of RhoG in the regulation of NPC proliferation. These observations contribute in part to the understanding of the physiological role of RhoG and the molecular mechanisms underlying cortical development.

MATERIALS AND METHODS

Plasmids and Short Hairpin RNAs

pCAG-EYFP (Saito and Nakatsuji, 2001) was used as a control. Myc-tagged wild-type RhoG (RhoG-WT), RhoG-V12, and RhoG-V12A37 generated previously (Katoh *et al.*, 2000) were inserted into pCAG-EYFP-CAG vector (Saito and Nakatsuji, 2001). pCAG-EYFP-U6 vector was constructed by inserting a fragment encoding the human U6 promoter into pCAG-EYFP (Iwasato *et al.*, 2007). The short hairpin RNAs (shRNAs) for RhoG were designed to target 19 nucleotides of the mouse RhoG transcript (shRG-A: nucleotides 48-66, 5′-GACGTGCCTTCTCATCTGC-3′ and shRG-B: nucleotides 94-112, 5′-TA-CATCCCCACTGTGTTTG-3′). A control shRNA for luciferase was designed as described previously (Fujito *et al.*, 2005; Yamaki *et al.*, 2007). These plasmids have CAG promoter that is efficient to introduce genes into mammalian cells (Niwa *et al.*, 1991). pEF-BOS-Myc-RhoG-WT vector generated previously (Katoh *et al.*, 2000) is used for the rescue experiment.

Antibodies

We used the following primary antibodies: rabbit polyclonal anti-GFP (1:1000, Molecular Probes, Eugene, OR), rabbit polyclonal anti-Ki67 (1:1000, Abcam, Cambridge MA), mouse monoclonal anti-Nestin (1:500, BD PharMingen), mouse monoclonal anti-BrdU (1:2000, BD Biosciences Pharmingen, San Diego, CA), mouse monoclonal anti-Tuj1 (1:3000, Covance, Madison, WI), mouse monoclonal anti-Myc (1:500, Santa Cruz Biotechnology, Santa Cruz, CA), mouse monoclonal anti-α-tubulin (1:1000, Sigma, St. Louis, MO), rabbit polyclonal anti-phospho Akt (Ser473) (1:1000, Cell Signaling Technology, Beverly, MA), and Alexa Fluor 488–conjugated anti-GFP (1:1000, Molecular Probes); and the secondary antibodies: Alexa Fluor 488–conjugated goat anti-rabbit IgG (1:1000, Molecular Probes), Alexa Fluor 555–conjugated goat anti-mouse IgG (1:3000, Molecular Probes), Alexa Fluor 594–conjugated goat anti-mouse IgG (1:3000, Molecular Probes), Alexa Fluor 594–conjugated goat anti-rabbit IgG (1:1000, Molecular Probes), Alexa Fluor 647–conjugated goat anti-rabbit IgG (1:1000, Molecular Probes), horseradish peroxidase (HRP)-conjugated goat anti-mouse IgG (1:3000, DAKO, Carpinteria, CA), and HRP-conjugated goat anti-rabbit IgG (1:1000, DAKO).

Tissue Preparation

Pregnant ICR mice were purchased from Japan SLC (Shizuoka, Japan), and treated in accordance with the guidelines for the Animal Care and Use Committee of the Graduate School of Biostudies at Kyoto University. Isolated embryonic day 12 (E12) embryos and brains were fixed in 4% paraformaldehyde (PFA) in phosphate-buffered saline (PBS) and then saturated with 30% sucrose in PBS overnight at 4°C. Embryos and brains were embedded in OCT compound (Sakura, Torrance, CA), frozen with dry ice, and stored at −80°C until use.

In Situ Hybridization

To obtain a specific riboprobe for mouse RhoG, the RhoG cDNA fragment corresponding to the nucleotide 1–400 was generated from mouse brain total RNA by using standard RT-PCR method (primers, 5′-TTTCTAGAATGCA-GAGCATCAAGTGTGT-3′ and 5′-TTCTCGAGGACCCTGCTCCTTGAG-GCGC-3′) and subcloned into pBluescript SK(+). The nucleotide sequence was confirmed using the ABI Prism 310 Genetic Analyzer (Applied Biosystems, Foster City, CA). Antisense and sense probes were synthesized in vitro transcription with T7 and T3 RNA polymerases from the XbaI- and XhoI-digested plasmid, respectively, and digoxigenin (DIG)-labeled by DIG RNA-labeling mix (Roche, Indianapolis, IN).

In situ hybridization was performed as described previously (Katoh *et al.*, 2006b). In brief, 40-μm-thick coronal sections were treated with 0.5 μg/ml proteinase K (Roche) for 3 min and then acetylated in acetic anhydride/triethanolamine-HCl for 10 min at room temperature. After prehybridization in hybridization buffer (50% deionized formamide, 5× SSC, 5× Denhardt's solution, 250 μg/ml salmon sperm DNA, and 250 μg/ml yeast tRNA) for 2 h, the sections were hybridized overnight at 55°C with the DIG-labeled anti-

sense or sense probe. After washing, the sections were blocked with 1% blocking reagent (Roche) for 1 h at room temperature and incubated with alkaline phosphatase–conjugated anti-DIG antibody (1:2000, Roche) overnight at 4°C. Antibody binding was detected with 5-bromo-4-chloro-3-indolylphosphate and nitroblue tetrazolium (Roche).

In Vivo Electroporation

In vivo electroporation was performed as described previously (Saito and Nakatsuji, 2001). In brief, timed pregnant ICR mice were deeply anesthetized, and the uterine horns carrying embryos were exposed through a midline abdominal incision. Two microliters of plasmid solutions (0.5–0.8 μg/μl diluted with saline) was injected into the lateral ventricle of the embryos using a micropipette made from a glass capillary. Electric pulses (50 ms at 950-ms intervals) were delivered five times with forceps-type electrodes (CUY650P5, Nepa Gene, Chiba, Japan) and an electroporator (CUY21EDIT, Nepa Gene) at 40 V for E13 or 50 V for E14. The uterine horns were then placed back into the abdominal cavity and the abdominal wall was sutured.

Immunohistochemistry and Immunocytochemistry

Frozen brains were sliced in 10-μm-thick coronal sections using a cryostat (CM3050S, Leica, Deerfield, IL). Sections were washed with PBS, permeabilized with 0.3% Triton X-100 in PBS for 15 min, and then blocked with PBS containing 1% blocking reagent (Roche), 1% goat serum, and 0.15% Triton X-100 for 1 h at room temperature. The sections were incubated with the primary antibodies for 24 h at 4°C. After five washes with PBS containing 0.1% Tween 20, the sections were incubated with the appropriate secondary antibodies for 24 h at 4°C. Then they were washed five times with PBS containing 0.1% Tween 20 and mounted using 90% glycerol containing 0.1% *p*-phenylenediamine dihydrochloride in PBS.

Cultured cells on coverslips were fixed with 4% PFA in PBS for 20 min and washed three times with PBS. The cells are permeabilized with 0.2% Triton X-100 in PBS for 10 min and blocked with 10% fatal bovine serum (FBS) in PBS for 1 h. Then they were incubated with primary antibodies overnight at 4°C, washed five times with PBS, and incubated with appropriate secondary antibodies. After five washes with PBS, the cells were treated with Hoechst 33258 for 5 min and mounted. Images were captured using a Nikon Eclipse E800 microscope and objectives equipped with a Leica DC350F digital camera (Melville, NY), and processed by ImageJ (http://rsb.info.nih.gov/ij/) and Photoshop (Adobe Systems, San Jose, CA).

BrdU Labeling and TUNEL Assay

For in vivo labeling, pregnant mice were injected intraperitoneally with BrdU dissolved in saline at 50 μg/g of body weight. The mice were either killed 30 min or 2 h after the injection for analysis of BrdU incorporation. For cell cycle exit analysis, the mice were killed 24 h after injection. For in vitro labeling, BrdU was added at a final concentration of 3 μg/ml to the medium, and cells were incubated for 3 h. To identify BrdU-incorporated cells, sections and cells were pretreated with 4N HCl in PBS for 10 min at room temperature before the application of anti-BrdU antibody. TUNEL (TdT-mediated dUTP-biotin nick end labeling) assay was performed using in situ cell death detection kit TMR red (Roche) according to the manufacturer's instruction. As a positive control, sections were pretreated with 10 U/ml DNase I for 10 min at room temperature.

NPC Primary Culture

Timed pregnant mice were killed, and embryos were removed. Embryonic cerebral cortices were dissected in ice-cold calcium- and magnesium-free HBSS. After incubated in HBSS with 0.25% trypsin and 0.1% DNase for 15 min at 37°C, the tissues were triturated mechanically with a pipette and dispersed in single cell in DMEM containing 4 mM L-glutamine, 100 U/ml penicillin, 0.1 mg/ml streptomycin, 1% B27 supplement (Invitrogen), 1% N2 supplement (Invitrogen), and 10 ng/ml basic FGF (Sigma). The cells were plated onto round 13-mm coverslips coated with 0.01 mg/ml poly-D-lysine at a density of 2×10^5 cells and cultured in the medium under the humidified conditions in 95% air and 5% CO_2 at 37°C. For the phosphatidylinositol 3-kinase (PI3K) inhibitor treatment, the medium was changed to fresh medium containing LY294002 (Calbiochem, La Jolla, CA) 3 h after plating.

Detection of Akt Phosphorylation

After E12 brains were dissected and NPCs were isolated, NPCs (3×10^6 cells) were electroporated before plating with mouse NSC nucleofector kit (Amaxa Biosystems, Gaithersburg, MD) according to the manufacturer's instructions. Electroporated cells were cultured in the DMEM/F12 (1:1, GIBCO, Rockville, MD) containing 1% N2 supplement, 10 ng/ml basic fibroblast growth factor (FGF), and 10 ng/ml epidermal growth factor (EGF) for 20 h under the humidified conditions in 95% air and 5% CO_2 at 37°C. Cells were then collected and lysed with 1× Laemmli sample buffer. The cell lysates were analyzed by SDS–PAGE and immunoblotting. Densitometry analysis was performed with ImageJ.
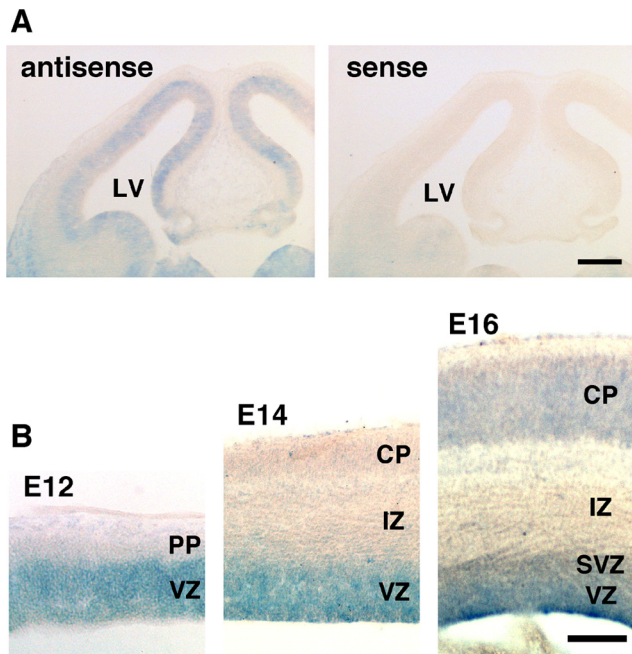
A

B

Figure 1. RhoG mRNA is expressed in the VZ. (A) In situ hybridization was performed with a RhoG-specific antisense (left) or sense (right) probe on a coronal section of the E12 mouse brain. (B) Highly magnified images of the E12, E14, and E16 cerebral cortices are shown. LV, lateral ventricle; PP, preplate; VZ, ventricular zone; SVZ, subventricular zone; IZ, intermediate zone; CP, cortical plate. Scale bars: (A) 200 μm; (B) 100 μm.

HEK293T Cell Culture and Transfection

HEK293T cells were cultured in DMEM containing 10% FBS, 4 mM L-glutamine, 100 U/ml penicillin, and 0.1 mg/ml streptomycin under the humidified conditions in 95% air and 5% CO_2 at 37°C. HEK293T cells were transfected with indicated expression vectors using Lipofectamine Plus (Invitrogen), according to the manufacturer's instructions.

Immunoblotting

Proteins were separated by SDS-PAGE and were electrophoretically transferred onto a polyvinylidene difluoride membrane (Millipore, Bedford, MA). The membrane was blocked with 3% low fat milk in Tris-buffered saline, and then incubated with primary antibodies. The primary antibodies were detected with HRP-conjugated secondary antibodies and a chemiluminescence detection kit (Chemi-Lumi One; Nacalai Tesque, Kyoto, Japan; ECL Plus Western Blotting Detection System; GE Healthcare, Waukesha, WI).

RESULTS

RhoG mRNA Is Expressed in the VZ at Early Stages of Cortical Development

Initially, we confirmed the expression of RhoG in the developing mouse brain. RT-PCR analyses on the mouse brain total RNA indicated that RhoG mRNA was expressed at all developmental stages (data not shown). To determine the precise distribution of RhoG mRNA in the early developing mouse brain, we performed in situ hybridization using a DIG-labeled riboprobe. In the (E12 brain, RhoG mRNA is expressed throughout the VZ (Figure 1A, left). This result is consistent with the previous experiment in the rat brain (Ishikawa *et al.*, 2002). No significant signal was detected in the section hybridized with a sense probe (Figure 1A, right). Focusing on the cerebral cortex, RhoG mRNA was detected in the VZ and the subventricular zone (SVZ) from E12 to E16 but neither in the preplate (PP), the IZ nor the CP at E12 and E14, although it was weakly detected in the

CP at E16 (Figure 1B). These results suggest that RhoG is expressed in the proliferative VZ/SVZ at early stages of cortical development.

Overexpression of Constitutively Active RhoG Promotes Cultured NPC Proliferation and BrdU Incorporation

Considering that RhoG mRNA was expressed in the VZ/SVZ, which is abundant in NPCs at the stages, we carried out in vivo electroporation, by which plasmids injected into the lateral ventricle can be introduced into the NPCs adjacent to the ventricular surface of dorsolateral cortex (Figure 2A). We used pCAG-EYFP (Control) as a control vector, and a wild-type RhoG expression vector, pCAG-EYFP-CAG-Myc-RhoG-WT (RhoG-WT), and a constitutively active RhoG expression vector, pCAG-EYFP-CAG-Myc-RhoG-V12 (RhoG-V12) in the following experiments. To investigate the involvement of RhoG in NPC proliferation, NPCs were dissociated from E14 mouse brains electroporated with control, RhoG-WT, or RhoG-V12 vector at E13 and cultured in vitro for 24 or 48 h (Figure 2A). After fixation, the numbers of EYFP-positive (EYFP$^+$) cells were counted, and the relative proliferation rate of EYFP$^+$ cells electroporated with RhoG-WT or RhoG-V12 was compared with that of cells electroporated with control vector. Although expression of RhoG-WT had little effect on the relative NPC proliferation rate, expression of RhoG-V12 led to a significant increase in the relative rate of NPC proliferation (Figure 2B).

To further investigate the role of RhoG in NPC proliferation, we performed short BrdU labeling. Twenty-four hours after in vivo electroporation with each expression vector, pregnant mice were injected intraperitoneally with BrdU solution and killed 30 min after injection. To count the precise number of cells, isolated brains from the embryos were dissociated into single cells and stained with anti-BrdU and anti-GFP (EYFP) antibodies and with Hoechst 33258 to stain nuclei (Figure 2C). When RhoG-V12 was electroporated, about twofold increase in the percentage of BrdU-incorporated cells was observed compared with that of control cells (Figure 2D). These results indicate that activation of RhoG promotes proliferation of NPCs. Next, we examined the effect of an effector domain mutant, RhoG-V12A37 on BrdU incorporation in NPCs. Previous studies have shown that RhoG-V12A37 has no ability to bind to its effector ELMO and to activate Rac1 (Katoh *et al.*, 2000, 2006a; Estrach *et al.*, 2002; Katoh and Negishi, 2003). However, the expression of RhoG-V12A37 also increased the percentage of BrdU-incorporated cells at a level similar to that of RhoG-V12-expressing cells (Figure 2, C and D). Therefore, these results indicate that activation of RhoG promotes NPC proliferation through a pathway independent of the ELMO-mediated activation of Rac1.

Knockdown of RhoG Reduces Cultured NPC Proliferation and BrdU Incorporation

To evaluate the involvement of intrinsic activity of RhoG in NPC proliferation, we performed RNA interference (RNAi)-mediated knockdown of RhoG. To visualize the shRNA-expressing cells, we used a double promoter vector, which expressed both enhanced yellow fluorescent protein (EYFP) and shRNA in the same cells (Figure 3A). We designed two shRNAs for two different regions of mouse RhoG cDNA (shRG-A and -B), and used a luciferase shRNA as a control shRNA (shLuc). To check the effectiveness of RhoG protein knockdown by these two shRNAs, Myc-tagged mouse RhoG and each shRNA expression vectors were coexpressed in HEK293T cells. These two shRNA expression vectors for RhoG effectively reduced the amount of exogenously expressed Myc-tagged
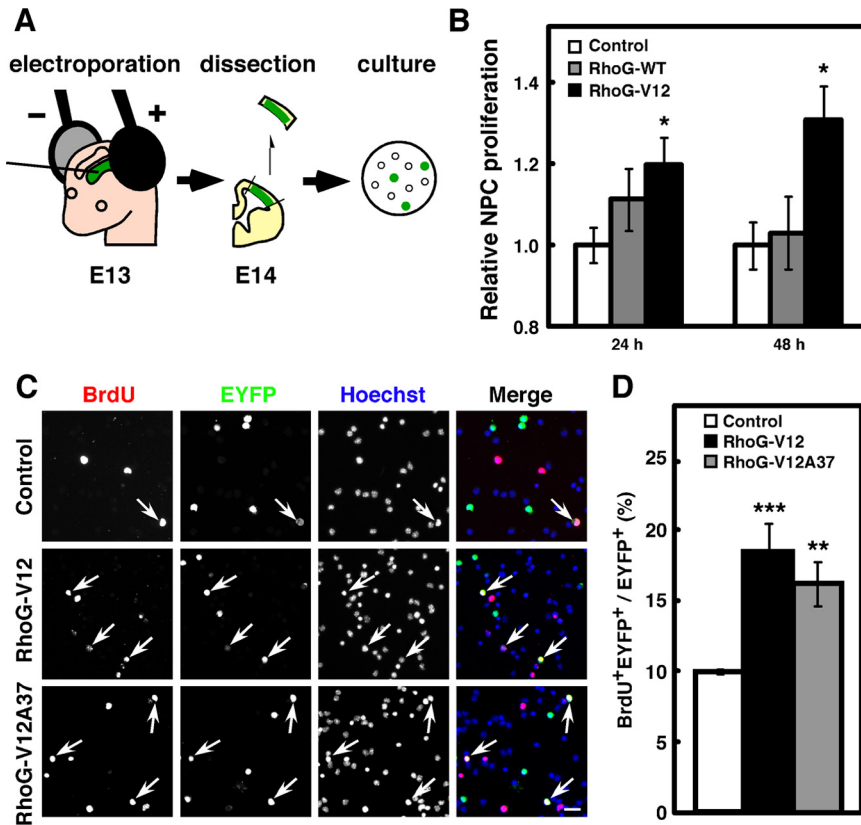
Figure 2. RhoG-V12 promotes proliferation of cultured NPCs. (A) Schematic drawing of the experimental procedure for primary culture after in vivo electroporation. (B) Twenty-four hours after control, RhoG-WT, or RhoG-V12 vector was electroporated at E13, the regions of cortices containing EYFP$^+$ cells were dissociated and dispersed on poly-D-lysine (PDL)-coated coverslips. Cells were fixed 3, 24, or 48 h after plating. Transfection efficiency was determined at 3 h after plating, and relative NPC proliferation was calculated by the percentages of EYFP$^+$ cells in total cells normalized for transfection efficiency and expressed relative to the value from Control-electroporated cells at the indicated time, which was set at 1.0. Control, n = 6; RhoG-WT, n = 5; RhoG-V12, n = 4. Values indicate means ± SEM; *p < 0.05 versus control (Student's *t* test). (C) Control, RhoG-V12, or RhoG-V12A37 vector was electroporated at E13 and labeled with BrdU for 30 min at E14. The regions of cortices containing EYFP$^+$ cells were dissociated and dispersed on PDL-coated coverslips. Cells were fixed 3 h after plating. Then cells were stained with anti-BrdU (red) and anti-GFP (green) antibodies. Nuclei were stained with Hoechst 33258 (blue). Arrows indicate BrdU$^+$EYFP$^+$ cells. Scale bar, 50 μm. (D) The numbers of BrdU$^+$EYFP$^+$ and EYFP$^+$ cells were counted, and the percentages of BrdU$^+$ cells in the total number of EYFP$^+$ cells were calculated. Control, n = 6; RhoG-V12, n = 6; RhoG-V12A37, n = 6. Values indicate means ± SEM; **p < 0.01, ***p < 0.001 versus control (Student's *t* test).

mouse RhoG in HEK293T cells, although shRG-B is less effective than shRG-A (Figure 3B). We could not examine the effect of the shRNAs on endogenous RhoG protein because we could not obtain antibodies for detecting specifically endogenous RhoG.

NPCs were dissociated from E14 brains electroporated with shLuc, shRG-A, or shRG-B at E13 and cultured in vitro for 24 or 48 h, and then the number of EYFP$^+$ cells was counted. Relative NPC proliferation rate of shRG-A– or -B-electroporated cells was significantly reduced compared with that of shLuc-electroporated cells (Figure 3C). We further examined the effect of shRG-A or -B on the BrdU incorporation in NPCs. When we performed in vivo BrdU labeling for 2 h, the percentage of BrdU-incorporated cells was significantly reduced in shRG-A–electroporated cells and also tended to be reduced in shRG-B–electroporated cells (Figure 3D). These results indicate that RhoG is involved in the regulation of NPC proliferation.

RhoG Regulates NPC Proliferation In Vivo

Next, to test in vivo requirement of RhoG activity on NPC proliferation, cortical sections of electroporated brains were stained with an antibody against the nuclear factor Ki67, which is expressed in proliferating cells from S- through M-phase. There was a significant increase in the percentage of Ki67$^+$ cells in RhoG-V12–electroporated brains compared with that in control brains (Figure 4, A and B). On the other hand, there was a significant decrease in the percentage of Ki67$^+$ cells in both shRG-A– and -B–electroporated brains compared with that in shLuc-electroporated brains (Figure 4, C and D). In addition, the reduction in the percentage of Ki67$^+$ cells by shRG-A electroporation was rescued by co-electroporation with hRhoG-WT, which was resistant to the

mouse RhoG shRNA (Figure 4, C and D). These results suggest that RhoG regulates NPC proliferation in vivo.

Knockdown of RhoG Does Not Increase NPC Apoptosis

Previous studies have shown that overexpression of constitutively active RhoG protects cells from apoptosis, whereas knockdown of RhoG promotes apoptosis (Murga *et al.*, 2002; Yamaki *et al.*, 2007). These observations indicate that RhoG is involved in cell survival. Therefore we examined whether or not the suppression of proliferation and BrdU incorporation of NPCs by knockdown of RhoG was due to the induction of apoptosis. Apoptotic cell death was detected by TUNEL assay. We performed the experimental validation by pretreating with DNase I as a positive control (Figure 5C). As a result, few TUNEL$^+$ cells were observed in the brain electroporated with RhoG shRNAs as well as with control luciferase shRNA (Figure 5, A and B), suggesting that suppression of proliferation and BrdU incorporation of NPCs by knockdown of RhoG is not due to the induction of apoptosis.

Overexpression of Constitutively Active RhoG Increased the Percentage of Nestin$^+$ NPCs

When control vector–electroporated cells were stained with an NPC marker Nestin, ~80% of the cells were Nestin$^+$ at E14 (Figure 6B), and when they were subsequently cultured in vitro, the percentage of Nestin$^+$ cells gradually decreased because Nestin$^+$ NPCs differentiated into neurons (Figure 6, A and B). Instead, most of the control cells were positive for a neuronal marker Tuj1 at 48 h after plating (Figure 6, C and D). However, the percentage of Nestin$^+$ cells in RhoG-V12–electroporated cells remained significantly higher than that in the control cells at 48 h after plating (Figure 6, A and B). In contrast, the percentages of Tuj1$^+$ cells remained lower
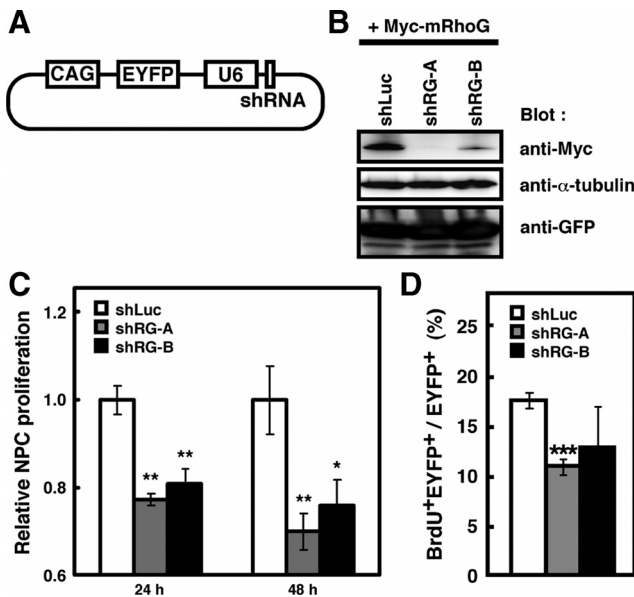
Figure 3. Knockdown of RhoG reduces cultured NPC proliferation and BrdU incorporation. (A) Structure of a double-promoter vector that possesses CAG and U6 promoters and can express both EYFP and shRNA in the same cell. (B) HEK 293T cells were transiently transfected with Myc-tagged mouse RhoG (Myc-mRhoG) and the indicated shRNA-expressing vectors. Cell lysates prepared 48 h after transfection were analyzed by immunoblotting with anti-Myc, anti-α-tubulin, and anti-GFP antibodies. (C) Twenty-four hours after electroporation of shRNA expression vectors for luciferase (shLuc), or RhoG (shRG-A or -B) at E13, the regions of cortices containing EYFP$^+$ cells were dissected and dispersed on PDL-coated coverslips. Cells were fixed 3, 24, or 48 h after plating. Relative NPC proliferation rate was determined as described in the legend to Figure 2. shLuc, n = 6; shRG-A, n = 5; shRG-B, n = 5. Values indicate means ± SEM; *p < 0.05, **p < 0.01 versus control (Student's t test). (D) shLuc, shRG-A, or -B vector was electroporated at E13, and labeled with BrdU for 2 h at E14. The regions of cortices containing EYFP$^+$ cells were dissociated and plated on PDL-coated coverslips. Three hours after plating, cells were stained with anti-BrdU and anti-GFP antibodies. Nuclei were stained with Hoechst 33258. The percentages of BrdU$^+$EYFP$^+$ in EYFP$^+$ cells were calculated as described in the legend to Figure 2. shLuc, n = 3; shRG-A, n = 3; shRG-B, n = 3. Values indicate means ± SEM; ***p < 0.001 versus shLuc (Student's t test).

(Figure 6, C and D). In addition, we frequently observed Nestin$^+$ or Tuj1$^-$ cell clusters in RhoG-V12-electroporated cells (Figure 6, A, arrows, and C, arrowheads). On the other hand, expression of RhoG-WT or knockdown of RhoG did not significantly affect the percentages of Nestin$^+$ or Tuj1$^+$ cells (Figure 6, A–F). To further examine the involvement of RhoG in NPC differentiation, we determined the fraction exiting cell cycle in shRNA-electroporated brains referred to in the previous study by Sanada and Tsai (2005). Brains were electroporated with shRNA expression vectors at E14, pulse-labeled by BrdU at E15, and stained with antibodies against EYFP, BrdU, and Ki67 at E16. We estimated the fraction exiting the cell cycle representing the percentage of EYFP$^+$BrdU$^+$Ki67$^-$ cells in EYFP$^+$BrdU$^+$ cells. However, no significant difference is observed in the fraction exiting the cell cycle between control- and RhoG-shRNAs-electroporated brains (Figure 6G). Therefore, these results suggest that RhoG is not involved in the maintenance of undifferentiated state of NPCs and that the higher percentage of Nestin$^+$ cells by expression of RhoG-V12 may be due to the expansion of highly proliferative NPCs.
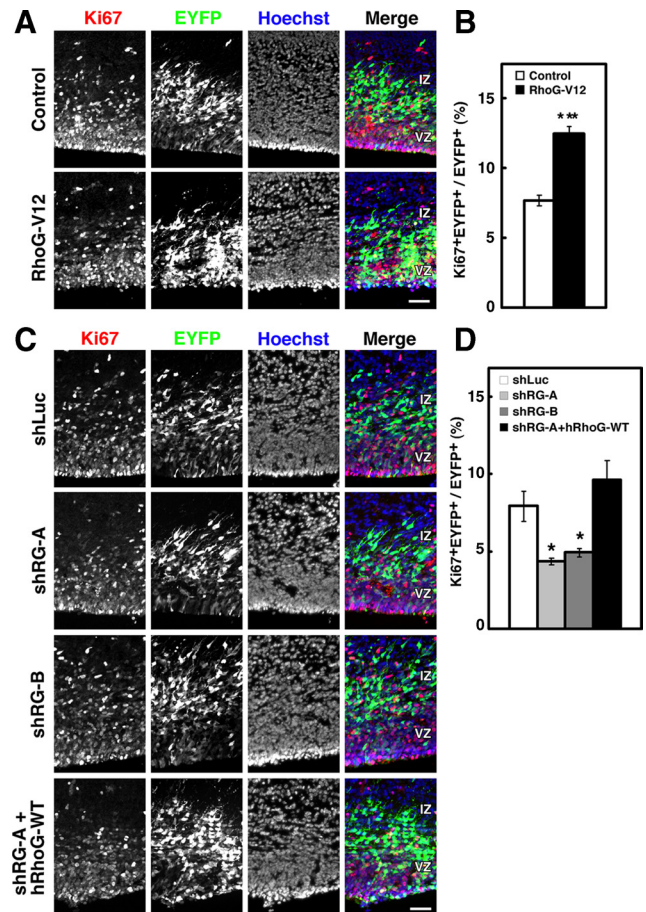

Figure 4. The percentage of Ki67$^+$ NPCs is increased by overexpression of RhoG-V12 and decreased by knockdown of RhoG in vivo. (A) Brains were fixed at E16 after electroporation with control or RhoG-V12 vector at E14, and cortical sections were stained with anti-Ki67 (red), anti-GFP (green), and Hoechst 33258 (blue). Scale bar, 50 μm. (B) Quantification of the percentages of Ki67$^+$ cells. Control, n = 3; RhoG-V12, n = 3. Values indicate means ± SEM; ***p < 0.001 versus control (Student's t test). (C) Brains were fixed at E16 after electroporation with shLuc, shRG-A, -B, or shRG-A together with human wild-type RhoG (hRhoG-WT) at E14 and stained with anti-Ki67 (red), anti-GFP (green), and Hoechst 33258 (blue). Scale bar, 50 μm. (D) Quantification of the percentages of Ki67$^+$ cells. shLuc, n = 3; shRG-A, n = 3; shRG-B, n = 3; shRG-A + hRhoG-WT, n = 3. Values indicate means ± SEM; *p < 0.05 versus shLuc (Student's t test).

The Regulation of NPC Proliferation by RhoG Requires PI3K Activity

RhoG has been shown to activate two signaling pathways, the ELMO-Dock180–mediated activation of Rac1 and the PI3K-mediated phosphorylation of Akt (Katoh and Negishi, 2003; Yamaki *et al.*, 2007). As shown above, RhoG-V12A37 promoted BrdU incorporation (Figure 2, C and D). RhoG-V12A37 is mutated in the effector domain of RhoG-V12 and cannot bind to ELMO, but can interact with PI3K and induce PI3K-mediated Akt phosphorylation (Yamaki *et al.*, 2007). Therefore, we investigated whether PI3K activity was required for the regulation of NPC proliferation by RhoG. RhoG-V12-electroporated cells were labeled with BrdU in the absence or presence of a PI3K inhibitor LY294002. The increase in the BrdU-incorporated cells by RhoG-V12 was suppressed by treatment with LY294002 (Figure 7A). In
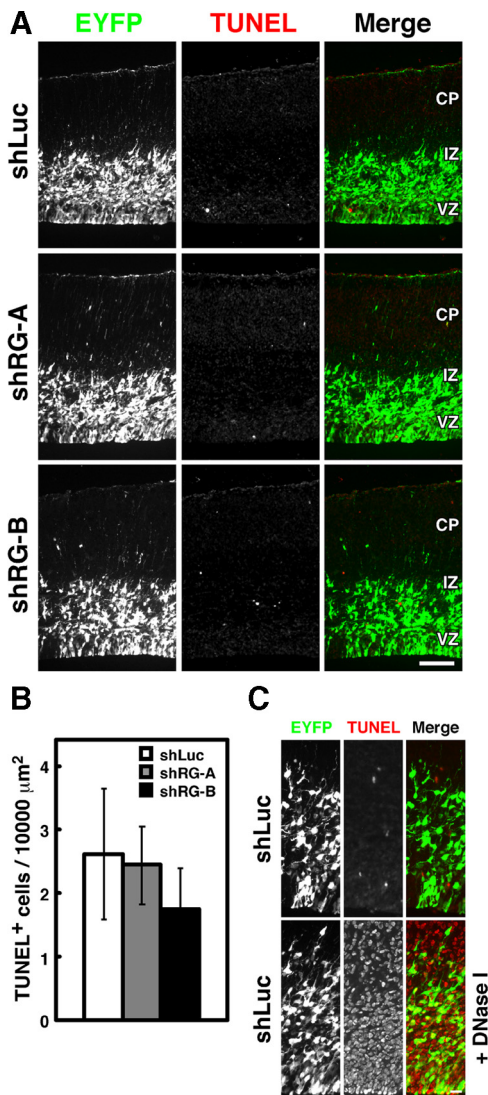
Figure 5. Knockdown of RhoG does not induce apoptosis. (A) Brains were fixed at E16 after electroporation with shLuc, shRG-A, or s-B vector at E14, and TUNEL assays were performed (red, middle). Cortical sections were stained with anti-GFP antibody (green, left). Scale bar, 100 μm. (B) Quantification of the numbers of TUNEL$^+$ cells per the area of 10,000 μm^2 of equally transfected cortical sections. shLuc, n = 3; shRG-A, n = 3; shRG-B, n = 3. Values indicate means $\pm$ SEM. (C) For data validation, shLuc-electroporated sections were pretreated with DNase I as a positive control. Scale bar, 20 μm.

addition, the RhoG-V12–induced increase in the percentage of Nestin$^+$ cells was also significantly suppressed by LY294002 treatment (Figure 7B). To examine whether RhoG triggers the activation of the PI3K pathway in NPCs, they were transfected with control or RhoG-V12 vector and phosphorylation of Akt was detected by immunoblotting. Expression of RhoG-V12 significantly increased the level of phosphorylated Akt (Figure 7C). Thus, these results indicate that regulation of NPC proliferation by RhoG is mediated by PI3K activity.

DISCUSSION

Regulation of NPC proliferation is an important process during the cortical development. To maintain the correct

size of neural progenitor pool and generate proper number of neurons, these processes are regulated spatially and temporally by a variety of molecules. To date, researchers have carried out intensive research about the regulation of extracellular factors such as EGF, FGF, Wnt, and Shh, and their receptors in NPC proliferation. On the other hand, it is well known that transcriptional regulators including *bHLH, Sox, Rb,* and *polycomb* genes participate in the NPC fate decision or proliferation. However, the mechanisms of intracellular signal transduction in the regulation of NPC proliferation are still largely unknown. In this study, we examined the role of RhoG in the developing cerebral cortex. RhoG is expressed in the VZ, which is a highly proliferative region at early stages of cortical development. Overexpression of constitutively active RhoG promoted NPC proliferation, whereas it was suppressed by RNAi-mediated knockdown of RhoG in vitro or in vivo. In addition, BrdU incorporation into NPCs was enhanced by constitutively active RhoG and suppressed by knockdown of RhoG. However, knockdown of RhoG affected neither the percentage of Nestin$^+$ cells nor the number of apoptotic cells, indicating that RhoG seems to regulate neither fate determination nor cell survival in NPCs. Taken together, we conclude that RhoG is a key positive regulator for proliferative activity of NPCs.

Previous studies using cell lines have provided some evidence that RhoG is involved in cell proliferation. In NIH3T3 cells, expression of constitutively active RhoG increases cell saturation density, and dominant negative RhoG-expressing cells increase doubling time at first and then grow normally, but stop growing at lower saturation density. Moreover, constitutively active RhoG potentiates Ras-induced focus formation (Roux *et al.,* 1997). Another study has shown that RhoG-depleted HeLa cells by RNAi are less proliferative (Yamaki *et al.,* 2007). On the other hand, the previous pathological study showed that RhoG is highly expressed in human breast cancer, and it is correlated with tumor malignancy (Jiang *et al.,* 2003). In addition, a comprehensive analysis of Rho family GTPases has shown that RhoG mRNA is highly expressed in mouse embryonic stem (ES) cells (Boureux *et al.,* 2007). Both tumor cells and ES cells possess highly proliferative activity. Thus, the expression level of RhoG may be correlated with the proliferative activity.

Previous studies have provided the knowledge about signaling pathways downstream of RhoG. It has been known that RhoG activates Rac1 and Cdc42 through distinct pathways and regulates actin cytoskeleton (Gauthier-Rouviére *et al.,* 1998; Wennerberg *et al.,* 2002). We have previously shown that RhoG activates Rac1 and promotes neurite outgrowth and cell migration by direct interaction with its specific effector ELMO and a Rac-specific guanine nucleotide exchange factor (GEF), Dock180 (Katoh and Negishi, 2003; Katoh *et al.,* 2006a). The RhoG-ELMO-Dock180–mediated activation of Rac1 is also involved in phagocytosis of apoptotic cells (deBakker *et al.,* 2004), and recent studies have shown that this pathway is utilized by bacterial invasion (Patel and Galán, 2006; Handa *et al.,* 2007; Roppenser *et al.,* 2009). However, our present study has shown that the ELMO-Dock180–mediated activation of Rac1 is dispensable for the promotion of NPC proliferation by RhoG because overexpression of an effector domain mutant of RhoG that cannot activate Rac1 also promoted BrdU incorporation at the level comparable to that of overexpression of constitutively active RhoG. Thus, Rac1 does not appear to be required for the RhoG-mediated NPC proliferation. On the other hand, RhoG interacts with the PI3K regulatory subunit, p85α, and induces phosphorylation of Akt. This pathway is involved in the resistance of UV-induced apoptosis
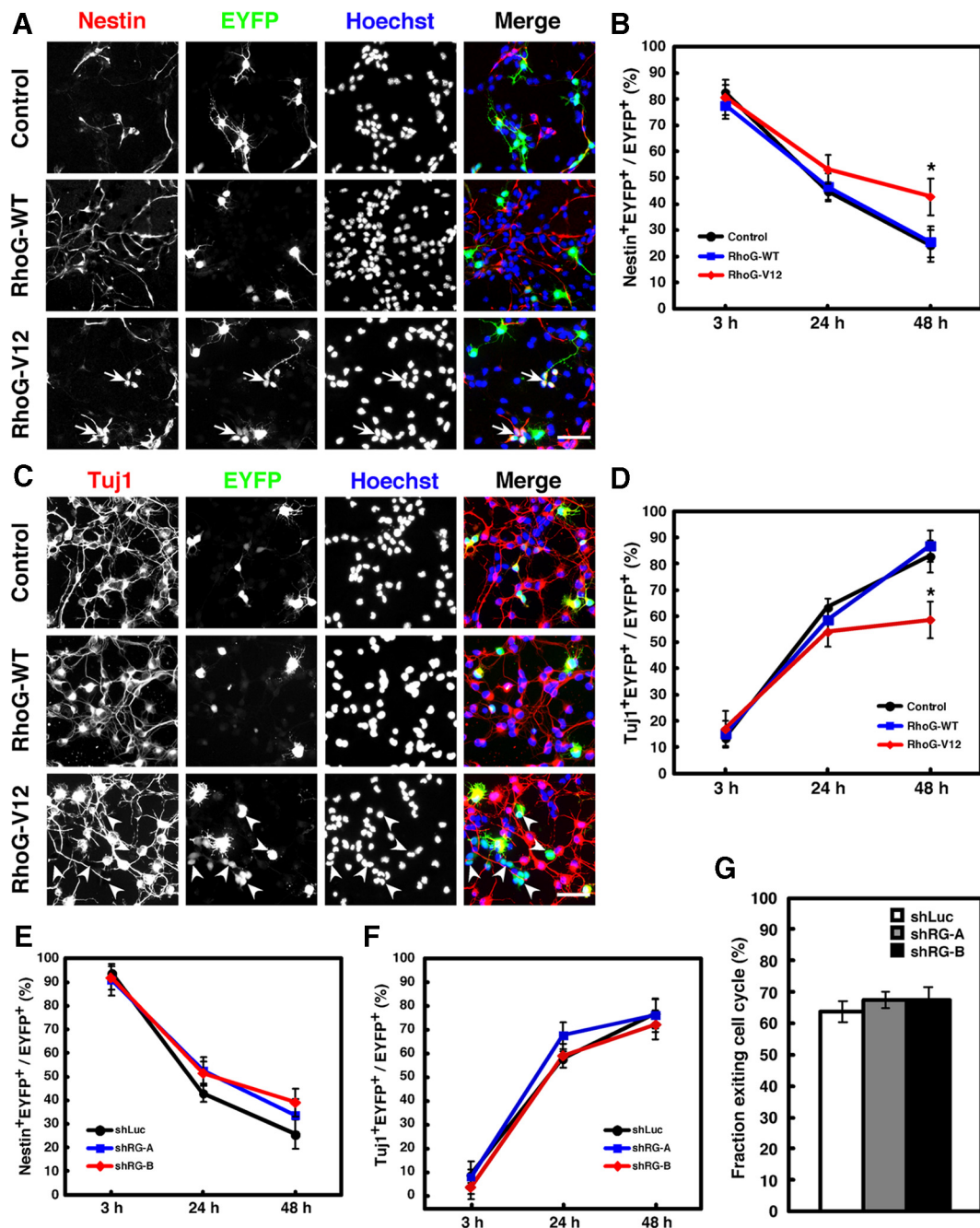
Figure 6. The percentage of Nestin$^+$ NPCs is increased by overexpression of RhoG-V12 but is not affected by knockdown of RhoG. (A) Cells electroporated with control, RhoG-WT, or RhoG-V12 vector at E13 were dispersed at E14 and stained with anti-Nestin (red), anti-GFP (green), and Hoechst 33258 (blue) after 48-h culture. Arrows indicate the Nestin$^+$ NPC clusters. Scale bar, 50 μm. (B) Twenty-four hours after control, RhoG-WT, or RhoG-V12 vector was electroporated at E13, the regions of cortices containing EYFP$^+$ cells were dissociated and dispersed on PDL-coated coverslips. Cells were fixed 3, 24, or 48 h after plating and stained with anti-Nestin antibody. The numbers of Nestin$^+$EYFP$^+$ and EYFP$^+$ cells were counted, and the percentages of Nestin$^+$ cells in the total number of EYFP$^+$ cells were calculated. Control, n = 9; RhoG-WT, n = 5; RhoG-V12, n = 6. Values indicate means ± SEM; *p < 0.05 (Student's t test). (C) Cells electroporated with control, RhoG-WT, or RhoG-V12 vector at E13 were dispersed at E14 and stained with anti-Tuj1 (red), anti-GFP (green), and Hoechst 33258 (blue) after 48-h culture. Arrowheads indicate the Tuj1$^-$ cell clusters. Scale bar, 50 μm. (D) Cells were cultured and fixed as described in B and then stained with anti-Tuj1 antibody. The numbers of Tuj1$^+$EYFP$^+$ and EYFP$^+$ cells were counted, and the percentages of Tuj1$^+$ cells in the total number of EYFP$^+$ cells were calculated. Control, n = 3; RhoG-WT, n = 3; RhoG-V12, n = 6. Values indicate means ± SEM; *p < 0.05 (Student's t test). (E) shLuc, shRG-A, or -B vector was electroporated at E13, and the percentages of Nestin$^+$ cells were quantified as described in B. shLuc, n = 6; shRG-A, n = 5; shRG-B, n = 5. Values indicate means ± SEM. (F) shLuc, shRG-A, or -B vector was electroporated at E13, and the percentages of Tuj1$^+$ cells were quantified as described in D. shLuc, n = 6; shRG-A, n = 6; shRG-B, n = 3. Values indicate means ± SEM. (G) shLuc, shRG-A, or -B vector was electroporated at E14, and brains were labeled with BrdU at E15 and fixed at E16. Cell cycle exit index indicate the percentages of EYFP$^+$BrdU$^+$Ki67$^-$ cells in EYFP$^+$BrdU$^+$ cells. shLuc, n = 3; shRG-A, n = 3; shRG-B, n = 3. Values indicate means ± SEM.
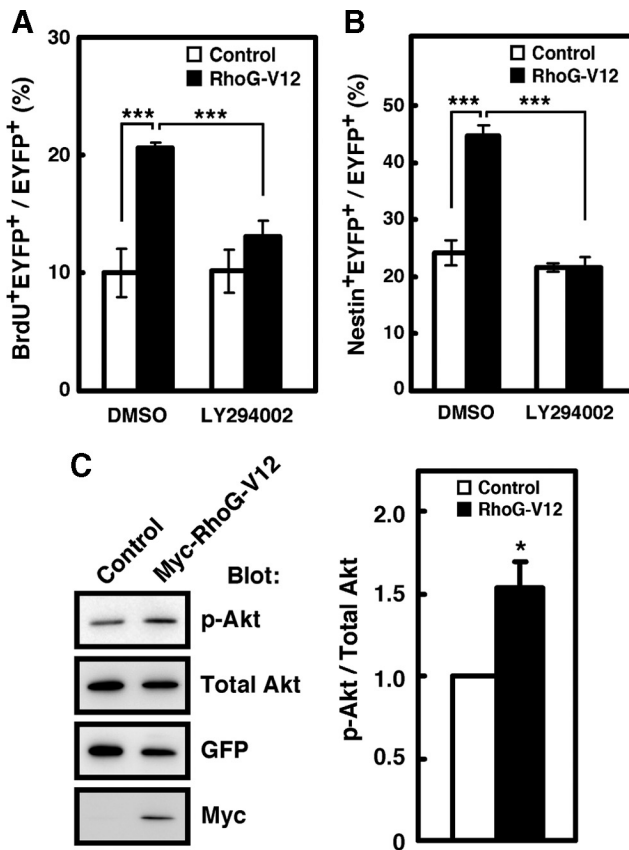
Figure 7. PI3K activity is required for the regulation of NPC proliferation by RhoG-V12. (A) Twenty-four hours after control or RhoG-V12 vector was electroporated at E13, the regions of cortices containing EYFP$^+$ cells were dissociated and dispersed on PDL-coated coverslips. Cells were cultured for 24 h in the absence or presence of LY294002 (20 μM) and labeled with BrdU for 3 h before fixation. Control, n = 6; RhoG-V12, n = 6. Values indicate means $\pm$ SEM; ***p $<$ 0.001 (Student's *t* test). (B) Twenty-four hours after control or RhoG-V12 vector was electroporated at E13, the regions of cortices containing EYFP$^+$ cells were dissociated and dispersed on PDL-coated coverslips. Cells were cultured for 48 h in the absense or presence of LY294002 (20 μM) and then fixed and stained with anti-Nestin antibody. Control, n = 6; RhoG-V12, n = 6. Values indicate means $\pm$ SEM; ***p $<$ 0.001 (Student's *t* test). (C) NPCs derived from E12 cortices transfected with control or RhoG-V12 were analyzed by immunoblotting with antibodies against phosphorylated Akt at serine 473 (p-Akt) and Akt (Total Akt). Quantitative analysis shows the amount of phosphorylated Akt normalized to the amount of total Akt in cell lysates. Value from control cells was arbitrarily set at 1.0. Values indicate means $\pm$ SEM of three independent experiments. *p $<$ 0.05 (Student's *t* test).

and anoikis, a form of apoptosis induced by cells detaching from extracellular matrix (Murga *et al.*, 2002; Yamaki *et al.*, 2007). In the present study, we show that a PI3K inhibitor LY294002 blocked the promotion of NPC proliferation by RhoG. Thus, these results suggest that RhoG regulates NPC proliferation via PI3K but not Rac1. From our results, LY294002 had little effect on the BrdU incorporation in control-electroporated cells, suggesting that this signaling pathway is not activated in NPCs in the culture condition. When LY294002 was intraventricularly injected, however, the percentage of BrdU$^+$ cells in the LY294002-injected brains was significantly reduced compared with that in the control brains (data not shown). This result indicates that PI3K activity is required for NPC proliferation in vivo.

PI3K is one of the key molecules that regulate cell proliferation in normal development and tumorigenesis. PI3K phosphorylates phosphatidylinositol-4,5-diphosphate and produces phosphatidylinositol-3,4,5-triphosphate, which activates Akt. PI3K/Akt signaling regulates cell proliferation through various kinds of signaling pathways (Vivanco and Sawyers, 2002; Takahashi *et al.*, 2005; Engelman *et al.*, 2006). For example, Akt promotes the G1/S transition by blocking FOXO-mediated transcription of cell cycle inhibitors. Akt also induces cell proliferation by mTOR/p70S6K/4E-BP–mediated protein synthesis. Another study showed that Akt can indirectly stabilize the cell cycle proteins such as c-Myc and cyclin D1 by inhibiting GSK3. Recently, Mairet-Coello *et al.* (2009) showed that PI3K/Akt activation by IGF-1 increased cyclin E and decreased p27Kip1 and p57Kip2 expression in cortical progenitors, suggesting that PI3K/Akt controls G1/S cell cycle progression in NPCs by regulating the transcription of cell cycle–related genes. In the present study, we showed that RhoG promotes NPC proliferation through PI3K pathway, and knockdown of RhoG results in a decrease in the percentage of BrdU$^+$ as well as Ki67$^+$ cells. On the other hand, the decrease in proliferation by knockdown of RhoG is neither due to the induction of apoptosis nor differentiation to the neuron. Taken together, RhoG may regulate G1/S cell cycle progression by modulating the transcription of cell cycle–related genes, and the decrease in proliferating NPCs upon RhoG knockdown may be due to delayed entry into the next cell cycle caused by slow progression of S-phase or the cell cycle arrest.

In the present study, we could not refer to the upstream regulators of RhoG in NPC proliferation. Currently, several molecules including SGEF, Trio, Kalirin, Vav, and PLEKHG6 are identified as GEFs for RhoG (Schuebel *et al.*, 1998; Movilla and Bustelo, 1999; Blangy *et al.*, 2000; May *et al.*, 2002; Vigorito *et al.*, 2003; Ellerbroek *et al.*, 2004; D'Angelo *et al.*, 2007). Although Kalirin is expressed predominantly in the nervous system and initiates new axon outgrowth mediated by RhoG in superior cervical ganglion neurons (May *et al.*, 2002), it is not expressed in the VZ during early cortical development (Hansel *et al.*, 2001). On the other hand, the regulatory mechanism of expression of RhoG is also largely unknown. However, given that RhoG was originally identified in fibroblast as a gene that is transcribed in a serum or growth factor stimulation–dependent manner (Vincent *et al.*, 1992), expression of RhoG may be spatially and/or temporally regulated by extracellular factors such as growth factors in the developing cerebral cortex, and may be linked to the cell cycle events. Our present study provides a novel physiological function of RhoG and a new aspect of the regulation of cortical development. However, there are still several questions that remain to be resolved, including how RhoG-PI3K signaling regulates cell proliferation, and that GEF modulates RhoG activity during corticogenesis. Further investigations are required for understanding the regulation of RhoG signaling during cortical development.

ACKNOWLEDGMENTS START HERE

REFERENCES

Blangy, A., Vignal, E., Schmidt, S., Debant, A., Gauthier-Rouvière, C., and Fort, P. (2000). TrioGEF1 controls Rac- and Cdc42-dependent cell structures through the direct activation of rhoG. J. Cell Sci. *113*, 729–739.

Boureux, A., Vignal, E., Faure, S., and Fort, P. (2007). Evolution of the rho family of ras-like GTPases in eukaryotes. Mol. Biol. Evol. *24*, 203–216.

Cappello, S., *et al.* (2006). The Rho-GTPase cdc42 regulates neural progenitor fate at the apical surface. Nat. Neurosci. *9*, 1099–1107.

Chen, L., Liao, G., Yang, L., Campbell, K., Nakafuku, M., Kuan, C. Y., and Zheng, Y. (2006). Cdc42 deficiency causes Sonic hedgehog-independent holoprosencephaly. Proc. Natl. Acad. Sci. USA *103*, 16520–16525.

Chen, L., Liao, G., Waclaw, R. R., Burns, K. A., Linquist, D., Campbell, K., Zheng, Y., and Kuan, C. Y. (2007). Rac1 controls the formation of midline commissures and the competency of tangential migration in ventral telencephalic neurons. J. Neurosci. *27*, 3884–3893.

Chen, L., Melendez, J., Campbell, K., Kuan, C. Y., and Zheng, Y. (2009). Rac1 deficiency in the forebrain results in neural progenitor reduction and microcephaly. Dev. Biol. *325*, 162–170.

D'Angelo, R., Aresta, S., Blangy, A., Del Maestro, L., Louvard, D., and Arpin, M. (2007). Interaction of ezrin with the novel guanine nucleotide exchange factor PLEKHG6 promotes RhoG-dependent apical cytoskeleton rearrangements in epithelial cells. Mol. Biol. Cell *18*, 4780–4793.

deBakker, C. D., *et al.* (2004). Phagocytosis of apoptotic cells is regulated by a UNC-73/TRIO-MIG-2/RhoG signaling module and armadillo repeats of CED-12/ELMO. Curr. Biol. *14*, 2208–2216.

Dehay, C., and Kennedy, H. (2007). Cell-cycle control and cortical development. Nat. Rev. Neurosci. *8*, 438–450.

Ellerbroek, S. M., Wennerberg, K., Arthur, W. T., Dunty, J. M., Bowman, D. R., DeMali, K. A., Der, C., and Burridge, K. (2004). SGEF, a RhoG guanine nucleotide exchange factor that stimulates macropinocytosis. Mol. Biol. Cell *15*, 3309–3319.

Engelman, J. A., Luo, J., and Cantley, L. C. (2006). The evolution of phosphatidylinositol 3-kinases as regulators of growth and metabolism. Nat. Rev. Genet. *7*, 606–619.

Estrach, S., Schmidt, S., Diriong, S., Penna, A., Blangy, A., Fort, P., and Debant, A. (2002). The Human Rho-GEF trio and its target GTPase RhoG are involved in the NGF pathway, leading to neurite outgrowth. Curr. Biol. *12*, 307–312.

Etienne-Manneville, S., and Hall, A. (2002). Rho GTPases in cell biology. Nature *420*, 629–635.

Fujito, T., Ikeda, W., Kakunaga, S., Minami, Y., Kajita, M., Sakamoto, Y., Monden, M., and Takai, Y. (2005). Inhibition of cell movement and proliferation by cell-cell contact-induced interaction of Necl-5 with nectin-3. J. Cell Biol. *171*, 165–173.

Gauthier-Rouvière, C., Vignal, E., Mériane, M., Roux, P., Montcourier, P., and Fort, P. (1998). RhoG GTPase controls a pathway that independently activates Rac1 and Cdc42Hs. Mol. Biol. Cell *9*, 1379–1394.

Götz, M., and Huttner, W. B. (2005). The cell biology of neurogenesis. Nat. Rev. Mol. Cell Biol. *6*, 777–788.

Govek, E. E., Newey, S. E., and Van Aelst, L. (2005). The role of the Rho GTPases in neuronal development. Genes Dev. *19*, 1–49.

Gupta, A., Tsai, L. H., and Wynshaw-Boris, A. (2002). Life is a journey: a genetic look at neocortical development. Nat. Rev. Genet. *3*, 342–355.

Handa, Y., Suzuki, M., Ohya, K., Iwai, H., Ishijima, N., Koleske, A. J., Fukui, Y., and Sasakawa, C. (2007). *Shigella* IpgB1 promotes bacterial entry through the ELMO-Dock180 machinery. Nat. Cell Biol. *9*, 121–128.

Hansel, D. E., Quiñones, M. E., Ronnett, G. V., and Eipper, B. A. (2001). Kalirin, a GDP/GTP exchange factor of the Dbl family, is localized to nerve, muscle, and endocrine tissue during embryonic rat development. J. Histochem. Cytochem. *49*, 833–844.

Heng, J. I., *et al.* (2008). Neurogenin 2 controls cortical neuron migration through regulation of Rnd2. Nature *455*, 114–118.

Hiramoto, K., Negishi, M., and Katoh, H. (2006). Dock4 is regulated by RhoG and promotes Rac-dependent cell migration. Exp. Cell Res. *312*, 4205–4216.

Ishikawa, Y., Katoh, H., Nakamura, K., Mori, K., and Negishi, M. (2002). Developmental changes in expression of small GTPase RhoG mRNA in the rat brain. Brain Res. Mol. Brain Res. *106*, 145–150.

Iwasato, T., *et al.* (2007). Rac-GAP alpha-Chimerin regulates motor-circuit formation as a key mediator of EphrinB3/EphA4 forward signaling. Cell *130*, 742–753.

Jaffe, A. B., and Hall, A. (2005). Rho GTPases: biochemistry and biology. Annu. Rev. Cell Dev. Biol. *21*, 247–269.

Jiang, W. G., Watkins, G., Lane, J., Cunnick, G. H., Douglas-Jones, A., Mokbel, K., and Mansel, R. E. (2003). Prognostic value of rho GTPases and rho guanine nucleotide dissociation inhibitors in human breast cancers. Clin. Cancer Res. *9*, 6432–6440.

Katoh, H., and Negishi, M. (2003). RhoG activates Rac1 by direct interaction with the Dock180-binding protein Elmo. Nature *424*, 461–464.

Katoh, H., Hiramoto, K., and Negishi, M. (2006a). Activation of Rac1 by RhoG regulates cell migration. J. Cell Sci. *119*, 56–65.

Katoh, H., Fujimoto, S., Ishida, C., Ishikawa, Y. and Negishi, M. (2006b). Differential distribution of ELMO1 and ELMO2 mRNAs in the developing mouse brain. Brain Res. *1073–1074*, 103–108.

Katoh, H., Yasui, H., Yamaguchi, Y., Aoki, J., Fujita, H., Mori, K., and Negishi, M. (2000). Small GTPase RhoG is a key regulator for neurite outgrowth in PC12 cells. Mol. Cell. Biol. *20*, 7378–7387.

Kawauchi, T., Chihama, K., Nabeshima, Y., and Hoshino, M. (2003). The in vivo roles of STEF/Tiam1, Rac1 and JNK in cortical neuronal migration. EMBO J. *22*, 4190–4201.

Konno, D., Yoshimura, S., Hori, K., Maruoka, H., and Sobue, K. (2005). Involvement of the phosphatidylinositol 3-kinase/rac1 and cdc42 pathways in radial migration of cortical neurons. J. Biol. Chem. *280*, 5082–5088.

Luo, L. (2000). Rho GTPases in neuronal morphogenesis. Nat. Rev. Neurosci. *1*, 173–180.

Mairet-Coello, G., Tury, A., and DiCicco-Bloom, E. (2009). Insulin-like growth factor-1 promotes G1/S cell cycle progression through bidirectional regulation of cyclins and cyclin-dependent kinase inhibitors via the phosphatidylinositol 3-kinase/Akt pathway in developing rat cerebral cortex. J. Neurosci. *29*, 775–788.

May, V., Schiller, M. R., Eipper, B. A., and Mains, R. E. (2002). Kalirin Dbl-homology guanine nucleotide exchange factor 1 domain initiates new axon outgrowths via RhoG-mediated mechanisms. J. Neurosci. *22*, 6980–6990.

Meller, J., Vidali, L., and Schwartz, M. A. (2008). Endogenous RhoG is dispensable for integrin-mediated cell spreading but contributes to Rac-independent migration. J. Cell Sci. *121*, 1981–1989.

Movilla, N., and Bustelo, X. R. (1999). Biological and regulatory properties of Vav-3, a new member of the Vav family of oncoproteins. Mol. Cell. Biol. *19*, 7870–7885.

Murga, C., Zohar, M., Teramoto, H., and Gutkind, J. S. (2002). Rac1 and RhoG promote cell survival by the activation of PI3K and Akt, independently of their ability to stimulate JNK and NF-kappaB. Oncogene *21*, 207–216.

Nakamura, K., Yamashita, Y., Tamamaki, N., Katoh, H., Kaneko, T., and Negishi, M. (2006). In vivo function of Rnd2 in the development of neocortical pyramidal neurons. Neurosci. Res. *54*, 149–153.

Nakaya, M., Tanaka, M., Okabe, Y., Hanayama, R., and Nagata, S. (2006). Opposite effects of rho family GTPases on engulfment of apoptotic cells by macrophages. J. Biol. Chem. *281*, 8836–8842.

Negishi, M., and Katoh, H. (2002). Rho family GTPases as key regulators for neuronal network formation. J. Biochem. *132*, 157–166.

Niwa, H., Yamamura, K., and Miyazaki, J. (1991). Efficient selection for high-expression transfectants with a novel eukaryotic vector. Gene *108*, 193–200.

Patel, J. C., and Galán, J. E. (2006). Differential activation and function of Rho GTPases during *Salmonella*-host cell interactions. J. Cell Biol. *175*, 453–463.

Roppenser, B., Röder, A., Hentschke, M., Ruckdeschel, K., and Aepfelbacher, M. (2009). *Yersinia enterocolitica* differentially modulates RhoG activity in host cells. J. Cell Sci. *122*, 696–705.

Roux, P., Gauthier-Rouvière, C., Doucet-Brutin, S., and Fort, P. (1997). The small GTPases Cdc42Hs, Rac1 and RhoG delineate Raf-independent pathways that cooperate to transform NIH3T3 cells. Curr. Biol. *7*, 629–637.

Saito, T., and Nakatsuji, N. (2001). Efficient gene transfer into the embryonic mouse brain using in vivo electroporation. Dev. Biol. *240*, 237–246.

Sanada, K., and Tsai, L. H. (2005). G protein betagamma subunits and AGS3 control spindle orientation and asymmetric cell fate of cerebral cortical progenitors. Cell *122*, 119–131.

Schuebel, K. E., Movilla, N., Rosa, J. L., and Bustelo, X. R. (1998). Phosphorylation-dependent and constitutive activation of Rho proteins by wild-type and oncogenic Vav-2. EMBO J. *17*, 6608–6621.

Takahashi, K., Murakami, M., and Yamanaka, S. (2005). Role of the phospho-inositide 3-kinase pathway in mouse embryonic stem (ES) cells. Biochem. Soc. Trans. *33*, 1522–1525.

Vigorito, E., Billadeu, D. D., Savoy, D., McAdam, S., Doody, G., Fort, P., and Turner, M. (2003). RhoG regulates gene expression and the actin cytoskeleton in lymphocytes. Oncogene *22*, 330–342.

Vincent, S., Jeanteur, P., and Fort, P. (1992). Growth-regulated expression of rhoG, a new member of the ras homolog gene family. Mol. Cell. Biol. *12*, 3138–3148.

Vivanco, I., and Sawyers, C. L. (2002). The phosphatidylinositol 3-kinase AKT pathway in human cancer. Nat. Rev. Cancer *2*, 489–501.

Wennerberg, K., Ellerbroek, S. M., Liu, R. Y., Karnoub, A. E., Burridge, K., and Der, C. J. (2002). RhoG signals in parallel with Rac1 and Cdc42. J. Biol. Chem. *277*, 47810–47817.

Yamaki, N., Negishi, M., and Katoh, H. (2007). RhoG regulates anoikis through a phosphatidylinositol 3-kinase-dependent mechanism. Exp. Cell Res. *313*, 2821–2832.